

Aquatic Biospheres On Temperate Planets Around Sun-like Stars And M-dwarfs

MANASVI LINGAM^{1,2} AND ABRAHAM LOEB²

¹*Department of Aerospace, Physics and Space Sciences, Florida Institute of Technology, Melbourne FL 32901, USA*

²*Institute for Theory and Computation, Harvard University, Cambridge MA 02138, USA*

ABSTRACT

Aquatic biospheres reliant on oxygenic photosynthesis are expected to play an important role on Earth-like planets with large-scale oceans insofar as carbon fixation (i.e., biosynthesis of organic compounds) is concerned. We investigate the properties of aquatic biospheres comprising Earth-like biota for habitable rocky planets orbiting Sun-like stars and late-type M-dwarfs such as TRAPPIST-1. In particular, we estimate how these characteristics evolve with the ambient ocean temperature (T_W), which is a key environmental variable. We show that many salient properties, such as the depth of the photosynthesis zone and the net primary productivity (i.e., the effective rate of carbon fixation), are sensitive to T_W , and eventually decline substantially as the ocean temperature is increased. We conclude by discussing the implications of our analysis for the past and future Earth, and exoplanets orbiting M-dwarfs.

1. INTRODUCTION

It is a well-known fact that the Earth's environment - its lithosphere, hydrosphere, atmosphere, and biosphere - has transformed greatly over time (Lunine 2013; Knoll 2015; Stüeken et al. 2020), and the same also applies to other terrestrial planets in our Solar system (Ehlmann et al. 2016; Kane et al. 2019). In tandem, there has been growing awareness of the fact that habitability is a multi-faceted and dynamic concept that depends on a number of variables aside from the existence of liquid water (Kasting 2012; Cockell et al. 2016; Shields et al. 2016; Lingam & Loeb 2019a); the latter criterion is commonly employed to demarcate the limits of the so-called habitable zone (Dole 1964; Hart 1979; Kasting et al. 1993; Kopparapu et al. 2013; Ramirez 2018).

One of the most crucial environmental parameters that regulates myriad biological processes, and thus the propensity for planetary habitability, is the ambient temperature (Cossins & Bowler 1987; Hochachka & Somero 2002; Angilletta 2009; Clarke 2017). To begin with, it has been thoroughly established that even modest deviations in the environmental temperature can trigger a multitude of subtle but devastating effects on ecosystems, as seen from the unfolding saga of anthropogenic global warming on Earth (Blois et al. 2013; Kolbert 2014; McCauley et al. 2015; Pacifici et al. 2015; Behrenfeld et al. 2016) as well as certain mass extinctions in the Phanerozoic (Hallam & Wignall 1997; Bambach 2006; Bond & Grasby 2017; Penn et al. 2018). On

a different note, there exists a large body of work on the thermal limits of life based on comprehensive experiments on thermophiles (Rothschild & Mancinelli 2001; McKay 2014; Clarke 2014; Merino et al. 2019). In recent times, some studies have employed the thermal limits for Earth-like complex life to assess the habitability of exoplanets (Silva et al. 2017; Murante et al. 2020).

Motivated by these facts, we will study how temperature impacts the prospects for aquatic photosynthesis on Earth-analogs.¹ Our reasons for choosing to investigate aquatic photosynthesis are twofold. First, the importance of photosynthesis is well-established from the standpoint of physics and biochemistry as stellar radiation is the most plentiful source of thermodynamic disequilibrium (Deamer & Weber 2010), and photosynthesis represents the dominant avenue for the biosynthesis of organic compounds on Earth (Bar-On et al. 2018).

In particular, we will focus on oxygenic photosynthesis because its electron donor (water) is available in plentiful supply, consequently ensuring that this mechanism is not stymied by the access to electron donors (Ward et al. 2019). Moreover, the advent of oxygenic photosynthesis is known to have profoundly altered Earth's geochemistry and biology (Lane 2002; Judson 2017). We will adopt the conventional range of $\lambda_{\min} = 400$ nm and $\lambda_{\max} = 700$ nm for oxygenic photosynthesis (Blankenship 2014, Chapter 1.2), known as photosynthetically

¹ By Earth-analogs, we refer to rocky planets that are sufficiently similar to Earth insofar as their geological, physical, and chemical properties are concerned.

active radiation (PAR).² We will not tackle the possibility of multi-photon schemes that might elevate λ_{\max} to longer wavelengths (Wolstencroft & Raven 2002; Kiang et al. 2007; Lingam & Loeb 2019b), because their efficacy has not been adequately established.

The second reason as to why we tackle aquatic photosynthesis stems from the fact oceans contribute nearly half to the overall NPP of Earth (Field et al. 1998). In fact, Earth was mostly composed of oceans (i.e., virtually no large landmasses) for some fraction of its history (Iizuka et al. 2010; Arndt & Nisbet 2012), implying that aquatic photosynthesis would have played an even more significant role in that case. A few theoretical models have even proposed that continents only emerged in late-Archean era at 2.5 Gya (Flament et al. 2008), and this conjecture seems to be compatible with the recent analysis of oxygen-18 isotope data from the Pilbara Craton of Western Australia (Johnson & Wing 2020).

Looking beyond Earth, statistical analyses of exoplanets indicate that a substantial fraction of super-Earths are rich in volatiles (Rogers 2015; Wolfgang & Lopez 2015; Chen & Kipping 2017; Zeng et al. 2018; Jin & Mordasini 2018). In particular, some of the Earth-sized planets in the famous TRAPPIST-1 system (Gillon et al. 2017) may fall under this category, with the water fraction potentially reaching values as high as $\sim 10\%$ by mass (Grimm et al. 2018; Unterborn et al. 2018; Dorn et al. 2018). The habitability of ocean planets (also called water worlds), which are wholly devoid of continents (Kuchner 2003; Léger et al. 2004), has been analyzed from multiple standpoints (Cowan & Abbot 2014; Goldblatt 2015; Noack et al. 2017; Kite & Ford 2018; Ramirez & Levi 2018; Lingam & Loeb 2019c). A fair amount of attention has also been devoted to oceanographic phenomena such as circulation patterns and nutrient upwelling (Hu & Yang 2014; Cullum & Stevens 2016; Lingam & Loeb 2018a; Yang et al. 2019; Checlair et al. 2019; Del Genio et al. 2019; Olson et al. 2020; Salazar et al. 2020) on such worlds. However, a detailed treatment of the salient characteristics of aquatic photosynthesis remains missing for the most part.

The outline of the paper is as follows. We describe some of the basic tools needed to facilitate our analysis in Sec. 2. We follow this up by calculating how the properties of aquatic photosynthesis such as the compensation depth and the net primary productivity (NPP) vary with the ocean temperature in Sec. 3. Next, we delineate the ramifications arising from our modeling for Earth and M-dwarf exoplanets in Sec. 4, and we conclude with a synopsis of our central findings in Sec. 5.

² To be precise, oxygenic photosynthesis can operate at wavelengths of 350-750 nm (Chen & Blankenship 2011; Nürnberg et al. 2018), but the canonical choice of the PAR range delineated above does not alter our subsequent results significantly.

2. MATHEMATICAL PRELIMINARIES

In order to study the basic characteristics of aquatic photosynthesis vis-à-vis their dependence on the average ocean temperature (T_W), we hold all parameters (biological, geological and astrophysical) identical to that of Earth. We consider two different Earth-analogs hereafter: one around a solar twin (Planet G) and the other around a late-type M-dwarf (Planet M) with effective temperatures of $T_{\odot} = 5780$ K and $T = 2500$ K, respectively; the latter temperature has been chosen to closely resemble that of TRAPPIST-1 (Delrez et al. 2018). The reason for doing so is that Sun-like stars are considered “safe” targets for biosignature searches (Kasting et al. 1993; Heller & Armstrong 2014; Lingam & Loeb 2018b), whereas the habitability of M-dwarf exoplanets, especially those orbiting active stars, remains subject to many ambiguities (Tarter et al. 2007; Scalo et al. 2007; Shields et al. 2016; Lingam & Loeb 2019a).

In what follows, we draw upon two major simplifying assumptions. First, we model the star as an idealized black body with an effective temperature of T . Second, we account for the attenuation of PAR after the passage through the atmosphere by introducing a fudge factor. While neither of these simplifications are entirely realistic, the global results are known to deviate from more realistic models and data by a factor of only < 1.5 for the most part (Lingam & Loeb 2020).³ The reason for this reasonable degree of accuracy stems from the fact that most of the basic quantities we compute hereafter exhibit a weak (i.e., semi-logarithmic) dependence on the two assumptions outlined above.

As we are dealing with Earth-analogs, the stellar flux at the planet’s location is taken to be $S_{\oplus} \approx 1360$ W/m². At the substellar point on the planet, the photon flux density (\mathcal{N}_{\max}) at the top of the atmosphere is given by

$$\mathcal{N}_{\max}(\lambda) \approx n_{\lambda} \left(\frac{R_{\star}}{d_{\star}} \right)^2, \quad (1)$$

with R_{\star} and d_{\star} constituting the stellar and orbital radius, respectively, whereas n_{λ} is the photon flux density of the star at its surface. The black body brightness B_{λ} is invoked to yield

$$n_{\lambda} = \frac{B_{\lambda}}{(hc/\lambda)} = \frac{2c}{\lambda^4} \left[\exp \left(\frac{hc}{\lambda k_B T} \right) - 1 \right]^{-1}, \quad (2)$$

where λ is the photon wavelength. As we have assumed the stellar flux is equal to S_{\oplus} for the Earth-analogs, we

³ In fact, the spatial heterogeneity inherent to oceans are known to introduce local variations that are more than an order of magnitude greater than this factor (Behrenfeld et al. 2005), owing to which the estimates in Lingam & Loeb (2020) can be regarded as fairly accurate global values.

can express d_\star as follows:

$$d_\star = \sqrt{\frac{L_\star}{4\pi S_\oplus}} \quad (3)$$

where the stellar luminosity (L_\star) is given by $L_\star = 4\pi\sigma R_\star^2 T^4$. After employing this relation in (1), we find that \mathcal{N}_{\max} transforms into

$$\mathcal{N}_{\max}(\lambda) \approx \frac{n_\lambda S_\oplus}{\sigma T^4}. \quad (4)$$

It is, however, necessary to recognize that \mathcal{N}_{\max} constitutes an upper bound for the photon flux density at the surface for two reasons. First, this photon flux density is calculated at the zenith, and therefore ignores the fact that a given location will not always correspond to the substellar point. Second, the effects of clouds and atmospheric attenuation are neglected. Hence, a more viable expression for the photon flux density at the planet's surface (\mathcal{N}_{avg}) is given by

$$\mathcal{N}_{\text{avg}}(\lambda) \approx \mathcal{N}_{\max}(\lambda) \cdot f_I \cdot f_{\text{CL}}, \quad (5)$$

with f_{CL} embodying the total atmospheric attenuation (Sarmiento & Gruber 2006, Chapter 4.2), and f_I quantifying the average intensity of light at a given location as a fraction of the intensity at the substellar point. Henceforth, we adopt $f_A \equiv f_I \cdot f_{\text{CL}} \approx 0.2$ to maintain compatibility with Earth's parameters (Sarmiento & Gruber 2006, Chapter 4.3); altering this fraction by a factor of order unity does not change our results significantly due to the logarithmic dependence alluded to earlier in this section (Lingam & Loeb 2020). With this choice of f_A , it should be noted that $\mathcal{N}_{\text{avg}}(\lambda) \approx 0.2\mathcal{N}_{\max}(\lambda)$.

Given the photon flux density, denoted by $\mathcal{N}_0(\lambda)$, at the surface, we are in a position to calculate the photon flux \mathcal{F} at a depth z below the surface of the ocean. This quantity is found by convolving $\mathcal{N}_0(\lambda)$ and the vertical attenuation coefficient K in the oceans, thus yielding

$$\mathcal{F}(z) \approx \int_{\lambda_{\min}}^{\lambda_{\max}} \mathcal{N}_0(\lambda) \exp(-Kz) d\lambda. \quad (6)$$

It should be noted that $\mathcal{N}_0(\lambda)$ is equal to \mathcal{N}_{\max} or \mathcal{N}_{avg} , depending on what scenario we wish to analyze. Now, let us turn our attention to K , which we shall rewrite as $K = K_W + K_I$ (Kirk 2011, Chapter 9.5). The first term (K_W) is the attenuation coefficient associated with water whereas K_I accounts for the attenuation stemming from impurities as well as biota. In order to tackle K_W , we begin by noting that it has been tabulated as a function of λ in many sources (Hale & Querry 1973; Kou et al. 1993; Litjens et al. 1999). Based on the data taken from Pope & Fry (1997, Table 3), the following simple exponential fit was employed by Lingam & Loeb (2020) across the PAR range:

$$K_{W,22} \approx 1.4 \times 10^{-5} \text{ m}^{-1} \exp(\lambda \cdot 1.54 \times 10^7 \text{ m}^{-1}), \quad (7)$$

although it is essential to recognize that the data had been collected at 22 °C (Pope & Fry 1997, Table 3). In general, K_W is not only dependent on λ but also on T_W . The ocean temperature in turn varies with depth, but it only changes by a few K in the zone where photosynthesis occurs (Pawlowicz 2013). Hence, we shall treat T_W as being roughly constant, enabling us to model it as a free parameter in the model. In order to account for the dependence on T_W , we employ the linear temperature scaling that has been confirmed by a number of empirical studies (Langford et al. 2001; Sullivan et al. 2006; Röttgers et al. 2014), enabling us to write

$$K_W(T_W, \lambda) = K_{W,22} + \alpha(\lambda)\Delta T_{22}, \quad (8)$$

where $\alpha(\lambda)$ represents the wavelength-dependent temperature coefficient (units of $\text{m}^{-1} \text{ K}^{-1}$), and $\Delta T_{22} = T_W - 295$ represents the deviation from the standard water temperature of 22 °C used for calculating $K_{W,22}$.

For the PAR range considered herein, the second term on the right-hand-side of the above expression is always much smaller than the first term provided that ΔT_{22} is $\mathcal{O}(10)$ K. This condition arises because α is nearly zero across the PAR range ($\lesssim 10^{-3} \text{ m}^{-1} \text{ K}^{-1}$), as can be verified by comparing Röttgers et al. (2014, Figure 5) and Sullivan et al. (2006, Table 1) with Pope & Fry (1997, Table 3). Apart from the temperature dependence, we note that K_W also exhibits a dependence on the salinity, which is expected to vary from one ocean to another. However, we have implicitly held the salinity fixed to that of the global value of Earth's oceans. More importantly, the salinity dependence is weak across the PAR range, as shown by experimental studies (Sullivan et al. 2006; Röttgers et al. 2014).

Next, we turn our attention to the other attenuation coefficient K_I . If one considers the case with pure water, i.e., amounting to $K_I \rightarrow 0$, it follows that \mathcal{F} is maximized for a given depth *ceteris paribus*. In a more realistic setting, however, we shall adopt $K_I \approx 0.08 \text{ m}^{-1}$ to maintain consistency with the typical attenuation coefficient of Earth's oceans (Sarmiento & Gruber 2006, Chapter 4.2). In actuality, K_I will also be a function of wavelength and temperature, but the exact dependence is dictated by complex oceanographic and biological (e.g., density of photoautotrophs) factors, owing to which we have opted for a constant value.

At this stage, it is worth recapitulating the two broad scenarios we shall be considering. The first corresponds to the ideal case where the star is at the substellar point, and there is no attenuation because of the atmosphere and oceanic impurities. In other words, we employ $\mathcal{N}_0(\lambda) = \mathcal{N}_{\max}$ and $K = K_W$, and introduce the superscript "I" (i.e., ideal). This case was studied extensively by Ritchie et al. (2018), albeit with an exclusive focus on Earth and Proxima b. The second case accounts for time-averaged stellar flux and the existence of biological attenuation. Here, we select $\mathcal{N}_0(\lambda) = \mathcal{N}_{\text{avg}}$, $K = K_W + K_I$ and the finite value of K_I defined in

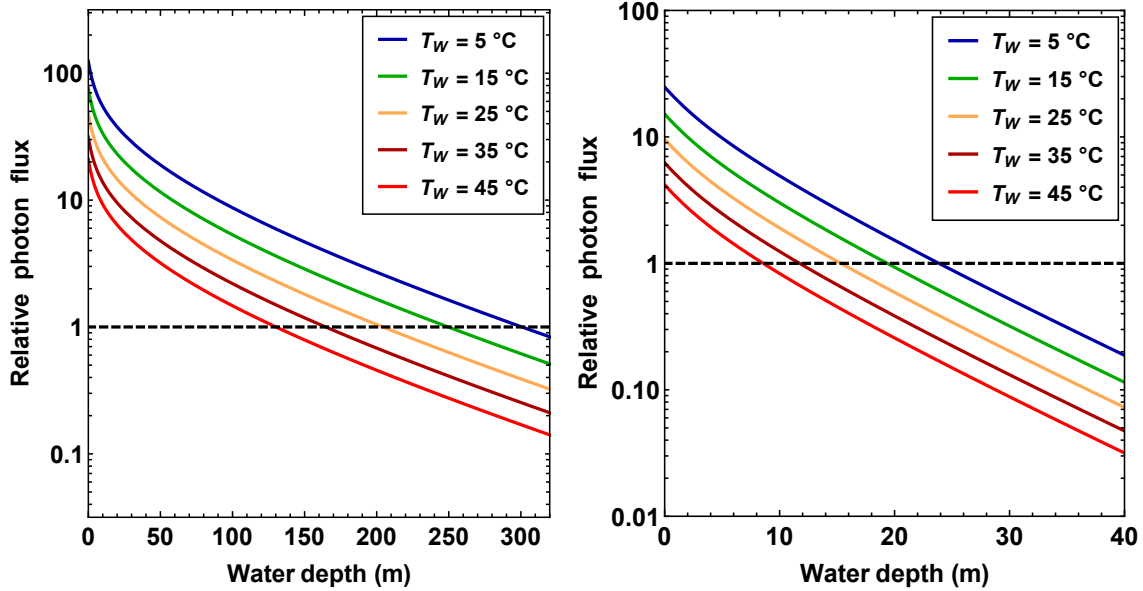


Figure 1. In both panels, the photon flux in units of the compensation flux (\mathcal{F}_C) is shown for an Earth-analog orbiting a solar twin (Planet G) as a function of the depth; the compensation flux specifies the photon flux at which net growth of the organism is not feasible. The various curves correspond to different choices of the global ocean temperature, and the intersection points of the various curves with the dashed horizontal line yield the compensation depths. In the left panel, the optimistic case with minimal attenuation and maximum incident stellar flux is illustrated. In the right panel, the realistic case that duly accounts for both these is depicted.

the prior paragraph, and label it using the superscript “R” (i.e., realistic). For each of these two scenarios, we consider two different Earth-analogs (Planets E & M) delineated at the beginning of this section.

In our subsequent analysis, we will draw upon the basic physiological properties of the dominant phytoplankton species on Earth. While this line of reasoning is undoubtedly parochial, we note that Earth-based organisms are commonly used as proxies in numerous astrobiological contexts ranging from extremophiles and microbial ecosystems in the oceans of icy moons (Chyba & Hand 2001; Rothschild & Mancinelli 2001; Merino et al. 2019; Lingam & Loeb 2019d) to the limits of complex multicellular life on exoplanets (Silva et al. 2017; Schwieterman et al. 2019; Lingam 2020; Ramirez 2020). Furthermore, the choice of phytoplankton as putative biota is motivated by the fact that they are the major source of carbon fixation in the oceans of modern Earth (Field et al. 1998; Falkowski et al. 2004; Canfield et al. 2005; Raven 2009). Hence, by utilizing the prior framework, we are now equipped to analyze the prospects for Earth-like aquatic photosynthesis on other worlds characterized by different ocean temperatures.

3. CHARACTERISTICS OF AQUATIC BIOSPHERES

In this section, we examine how some of the salient properties of aquatic biospheres depend on the ocean temperature; in some cases, we also investigate the joint dependence on stellar and ocean temperatures.

3.1. Compensation depth

The definitions and significance of the *compensation* depth (Z_{CO}) and the *critical* depth (Z_{CR}) have been recognized since the mid-20th century Sverdrup et al. (1942); Sverdrup (1953), and these two concepts have been further discussed in Canfield et al. (2005); Mann & Lazier (2006); Falkowski & Raven (2007); Kirk (2011); Middelburg (2019). Broadly speaking, both of these quantities are important because they enable us to gauge the depths at which photosynthetic organisms can exist and/or give rise to tangible biosignatures. The euphotic zone depth, where the flux becomes 1% of its surface value, is another useful measure but it is divorced from biological properties altogether, and does not constitute a reliable metric for the extent of the photosynthesis zone on Earth (Banse 2004; Marra et al. 2014).

In order to calculate Z_{CO} , it is necessary to determine the location at which the flux is equal to the compensation flux \mathcal{F}_C . The latter is defined as the flux at which the rate of growth via photosynthesis is equal to the rate of respiration; in other words, at this depth, the net growth rate of the photoautotroph in question becomes equal to zero (Marshall & Orr 1928). The key point worth appreciating here is that \mathcal{F}_C is *not* constant even for a given organism because it is intrinsically temperature-dependent. Thus, our chief objective is to find a suitable function that will adequately describe the behavior of \mathcal{F}_C with respect to T_W .

In the classical model for the compensation flux, it is proportional to Γ_R/Γ_P - see Siegel et al. (2002, Equation 2) and Mann & Lazier (2006, Chapter 3) - with Γ_R and Γ_P signifying the rates of respiration and photosynthesis, respectively. Thus, if we know how these rates vary with temperature, one can duly formulate the expression for \mathcal{F}_C . The temperature dependence of these rates is subject to uncertainty and many different fitting functions have been considered. However, both the standard metabolic theory of ecology (Gillooly et al. 2001; Brown et al. 2004) and recent analysis of empirical data from Earth’s oceans (Kirchman 2018, Figure 3.3) predict that both these rates are well described by the well-known Arrhenius equation.

Hence, by utilizing the respective activation energies for these two processes (Regaudie-De-Gioux & Duarte 2012, Section 3), we end up with

$$\frac{\Gamma_R}{\Gamma_P} \propto \exp\left(-\frac{\Delta E}{k_B T_W}\right), \quad (9)$$

where $\Delta E \approx 0.34$ eV constitutes the “net” activation energy, i.e., the difference between the corresponding activation energies. An important point worth noting is that the above ansatz for Γ_R/Γ_P is monotonically increasing with temperature. It is very unlikely that this behavior would be obeyed *ad infinitum* because the Arrhenius equation breaks down beyond a certain temperature (Kingsolver 2009; Angilletta 2009; Schulte 2015). The issue, however, is that the optimum temperature, after which the trend reverses, is species-dependent (Clarke 2017; Corkrey et al. 2018), and is modulated to some degree by the environment(s) of the putative organisms. We will restrict ourselves to $273 < T_W < 323$ K, as this interval roughly overlaps with the temperature range of $280 < T_W < 322$ K studied in Barton et al. (2020, pg. 724). In that study, diverse marine phytoplankton were shown to obey (9) for a broad thermal range.

By utilizing the above relationships, the temperature dependence of \mathcal{F}_C is modeled as

$$\mathcal{F}_C \approx 10 \mu\text{mol m}^{-2} \text{s}^{-1} \mathcal{G}(T_W), \quad (10)$$

where we have introduced the auxiliary function

$$\mathcal{G}(T_W) \equiv \exp\left[13.6 \left(1 - \frac{T_0}{T_W}\right)\right], \quad (11)$$

with $T_0 \approx 289$ K representing the global surface temperature of Earth’s oceans.⁴ The constant of proportionality in (10) has been chosen as it represents the compensation flux for phytoplankton in Earth’s oceans within a factor of ~ 2 (Nelson & Smith 1991; Marra 2004; Mann & Lazier 2006; Regaudie-De-Gioux & Duarte 2010). By solving for $\mathcal{F}(z) = \mathcal{F}_C$, we are equipped to calculate

the compensation depth \mathcal{Z}_{CO} as a function of both the stellar temperature and ocean temperature.

In Fig. 1, the photon flux normalized by the compensation flux is plotted for an Earth-analog orbiting a solar twin (Planet G). The various curves correspond to different ocean temperatures. In both panels, we find that \mathcal{Z}_{CO} decreases with the temperature along expected lines. The physical reason for this trend is that the increase in the rate of respiration outpaces that of photosynthesis when the temperature is elevated, thereby ensuring that the location at which the two processes balance each other is shifted closer to the surface, i.e., leading to a reduction in \mathcal{Z}_{CO} .

We observe that the ocean temperature has a moderate effect on the magnitude of \mathcal{Z}_{CO} for both cases. In the ideal scenario (left panel), the compensation depth changes from $\mathcal{Z}_{CO}^{(I)} \approx 300$ m at $T_W = 5^\circ\text{C}$ to $\mathcal{Z}_{CO}^{(I)} \approx 130$ m at $T_W = 45^\circ\text{C}$. For the realistic case (right panel), the compensation depth evolves from $\mathcal{Z}_{CO}^{(R)} \approx 24$ m at $T_W = 5^\circ\text{C}$ to $\mathcal{Z}_{CO}^{(R)} \approx 8.5$ m at $T_W = 45^\circ\text{C}$. Thus, in both instances, we see a moderate variation in \mathcal{Z}_{CO} induced by the varying ocean temperature.

Fig. 2 is analogous to that of Fig. 1, except that the Earth-analog (Planet M) is situated around a late-type M-dwarf closely resembling TRAPPIST-1 insofar as its effective temperature is concerned. Even for this system, we observe a decrease in \mathcal{Z}_{CO} when T_W is increased, but the impact of this variable is both qualitatively and quantitatively different than for Planet G. For the ideal case (left panel), the compensation depth morphs from $\mathcal{Z}_{CO}^{(I)} \approx 26.5$ m at $T_W = 5^\circ\text{C}$ to $\mathcal{Z}_{CO}^{(I)} \approx 3.5$ m at $T_W = 45^\circ\text{C}$. Thus, in this case, we determine that the ocean temperature could influence the compensation depth by almost an order of magnitude.

However, an even more drastic result is observed for the realistic case, i.e., the right panel of Fig. 2. At $T_W = 5^\circ\text{C}$, we obtain $\mathcal{Z}_{CO}^{(R)} \approx 3$ m, but when we consider $T_W = 45^\circ\text{C}$ instead, we find $\mathcal{Z}_{CO}^{(R)} = 0$. This cutoff arises because the temperature increases the compensation point to the extent that it overshoots the incident photon flux at the ocean’s surface.⁵ In fact, we find that $\mathcal{F}_0 \equiv \mathcal{F}^{(R)}(z=0) < \mathcal{F}_C$ occurs for $T_W > 24^\circ\text{C}$, implying that ocean temperatures above this value are relatively unlikely to host phytoplankton-like biota on exoplanets orbiting stars like TRAPPIST-1.

Motivated by our finding, we define $\zeta \equiv \mathcal{F}_0/\mathcal{F}_C$ and study the regimes in which $\zeta < 1$ is valid; this criterion enables us to assess the conditions under which Earth-like oxygenic photoautotrophs have a low likelihood of existence. We only tackle the realistic case herein, as it permits $\zeta < 1$ to occur in the parameter space. The

⁴ <https://www.ncdc.noaa.gov/sotc/global/201913>

⁵ We reiterate that our analysis deals with Earth-like biota, and the results need not necessarily apply to putative oxygenic photoautotrophs in the oceans of M-dwarf exoplanets.

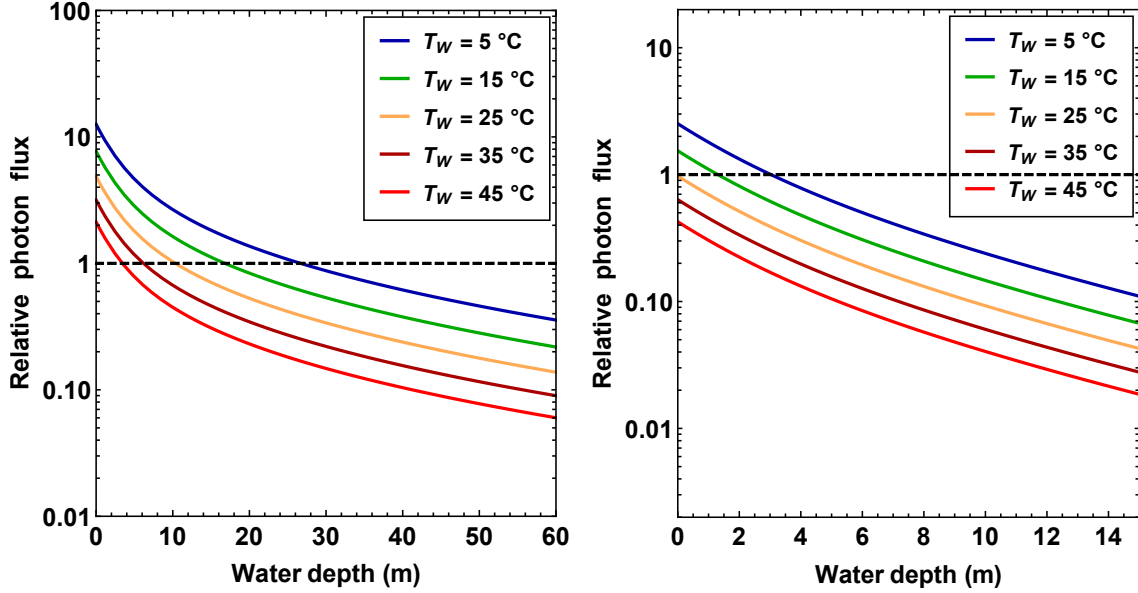


Figure 2. In both panels, the photon flux in units of the compensation flux (\mathcal{F}_C) is shown for an Earth-analog orbiting a late-type M-dwarf akin to TRAPPIST-1 (Planet M) as a function of the depth; the compensation flux specifies the photon flux at which net growth of the organism is not feasible. The various curves correspond to different choices of the global ocean temperature, and the intersection points of the various curves with the dashed horizontal line yield the compensation depths. In the left panel, the optimistic case with minimal attenuation and maximum incident stellar flux is illustrated. In the right panel, the realistic case that duly accounts for both these is depicted.

results are shown in Fig. 3, from which it is apparent that some of the smallest M-dwarfs might be incapable of hosting phytoplankton-like biota. In particular, for the maximal choice of $T_W = 50$ °C, we determine that stars with $T < 3150$ K may be ruled out in this category. Thus, in the presence of sufficiently warm oceans, exoplanets around late-type M-dwarfs could encounter difficulties in sustaining aquatic photosynthesizing organisms analogous to modern Earth.

3.2. Critical depth

The critical depth was introduced by Gran & Braarud (1935), and placed on a quantitative footing by Sverdrup (1953). It can be envisioned as a global version of the compensation depth. The critical depth is the location at which the *vertically integrated* net growth rate is zero, i.e., the integrated photosynthetic growth rate is equal to the integrated depletion rate because of respiration and other factors (Mann & Lazier 2006, Chapter 3). Photoautotrophs circulating in the region whose lower boundary is set by the critical depth are therefore, at least in principle, capable of survival.

The critical depth has the added advantage that it regulates the feasibility of phytoplankton blooms (Falkowski & Raven 2007), which have been posited to be an example of temporal biosignatures (Lingam & Loeb 2018a; Schwieterman et al. 2018). If the ocean mixed layer depth is greater than the critical layer depth, the initiation of phytoplankton blooms is rendered unlikely, and vice-versa (Mann & Lazier 2006, pg. 94).

Although the critical depth concept remains influential to this day (Obata et al. 1996; Siegel et al. 2002; Chiswell 2011; Fischer et al. 2014; Sathyendranath et al. 2015), it has been subjected to some criticism (Smetacek & Passow 1990; Behrenfeld 2010).

In order to calculate the critical depth (Z_{CR}), a number of different formulae have been delineated in the literature (Sverdrup 1953; Kirk 2011; Middelburg 2019). Most of the simpler models reduce to (Falkowski & Raven 2007, equation 9.7):

$$K Z_{CR} \approx \frac{\Gamma_P}{\Gamma_R}, \quad (12)$$

but they are correct only in the limiting case of $K = \text{const}$, which is manifestly invalid. The generalization of the above equation was adumbrated in Lingam & Loeb (2020), who eventually obtained

$$Z_{CR} \approx \left(\frac{\Gamma_R}{\Gamma_P} \right)^{-1} \frac{\int_{\lambda_{\min}}^{\lambda_{\max}} [\mathcal{N}_0(\lambda)/K(\lambda)] d\lambda}{\int_{\lambda_{\min}}^{\lambda_{\max}} \mathcal{N}_0(\lambda) d\lambda}. \quad (13)$$

It is, however, necessary to recognize that Γ_R/Γ_P has an intrinsic temperature dependence, as seen from (9). Hence, we combine (13) with (9), thereby yielding

$$Z_{CR} \approx \frac{3.36 \times 10^{-2}}{\mathcal{G}(T_W)} \frac{\int_{\lambda_{\min}}^{\lambda_{\max}} [\mathcal{N}_0(\lambda)/K(\lambda)] d\lambda}{\int_{\lambda_{\min}}^{\lambda_{\max}} \mathcal{N}_0(\lambda) d\lambda}, \quad (14)$$

where the normalization has been adopted based on the global value for phytoplankton in Earth's oceans

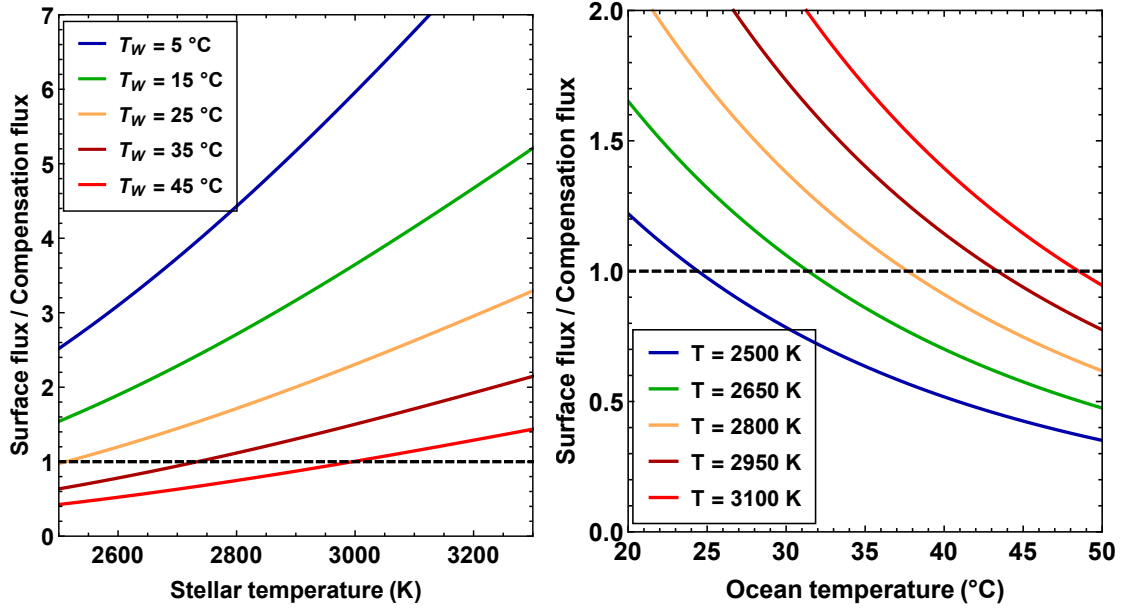


Figure 3. In both panels, the photon flux at the surface normalized by the compensation flux (denoted by ζ is depicted. Regions lying below the horizontal dashed line are relatively unlikely to host Earth-like biota in the oceans. Left panel: variation of ζ with stellar temperature (in K) shown for different ocean temperatures. Right panel: variation of ζ with ocean temperature (in °C) shown for different stellar temperatures.

(Sarmiento & Gruber 2006, Chapter 4.3). The parameters pertaining to the “R” scenario are adopted for the sake of comparison with prior empirical studies.

The temperature dependence of the critical depth is illustrated in Fig. 4. There are two points that emerge from scrutinizing this figure. For a fixed ocean temperature, the dependence on the stellar temperature is weak. This result is consistent with that of Lingam & Loeb (2020), and stems from the fact that net growth primarily takes place in the upper layers and thus compensates for the regions with $z > Z_{CO}$. However, when it comes to the ocean temperature, we immediately notice a much stronger variation of Z_{CR} . As we move across the entire ocean temperature range considered herein, we find that Z_{CR} varies by nearly an order of magnitude for any given stellar temperature. For instance, after we specify $T = T_{\odot}$, the critical depth evolves from $Z_{CR}^{(R)} \approx 416$ m at $T_W \approx 0$ °C to $Z_{CR}^{(R)} \approx 45$ m at $T_W \approx 50$ °C.

Therefore, it is conceivable that the ocean temperature plays a major role in regulating the critical depth on other worlds. In turn, this development suggests that T_W also acts as a key determinant of phenomena analogous to phytoplankton blooms, which may constitute viable temporal biosignatures.

3.3. Net primary productivity

The NPP is arguably one of the most crucial and informative property of a biosphere as it quantifies the net amount of organic carbon synthesized via biological pathways after accounting for losses due to respiration and other factors; we will express our results in units of

$\text{g C m}^{-2} \text{ h}^{-1}$ for the NPP. The NPP is a reliable measure of the amount of organic C generated via photosynthesis, as the latter constitutes the dominant carbon fixation pathway (Berg 2011; Knoll 2015; Judson 2017; Bar-On et al. 2018). A wide spectrum of models have been developed to model NPP, and comprehensive reviews can be found in Behrenfeld & Falkowski (1997) and Falkowski & Raven (2007, Chapter 9).

We make use of Field et al. (1998, Equation 3) to calculate the NPP, because this outwardly simple expression accounts for a number of environmental factors:

$$\text{NPP} = C_{\text{sur}} \cdot Z_{\text{CO}}^{(R)} \cdot f(\text{PAR}) \cdot P_{\text{opt}}(T_W), \quad (15)$$

where C_{sur} is the chlorophyll concentration at the surface, $f(\text{PAR})$ denotes the fraction of the water column up to $Z_{\text{CO}}^{(R)}$ where photosynthesis is light saturated, and $P_{\text{opt}}(T_W)$ is the optimal carbon fixation rate. There exists, however, an inherent crucial subtlety that needs to be spelt out here. In canonical versions of the above formula, $Z_{\text{CO}}^{(R)}$ is replaced by the euphotic zone depth. However, as noted in Field et al. (1998, pg. 237), the proper variable that ought to be deployed is the depth of the zone where positive NPP is feasible, which is congruent with the definition of the compensation depth. On Earth, the euphotic zone depth (Lee et al. 2007) and the compensation depth (Siegel et al. 2002; Middelburg 2019) are roughly equal to one another, but the same relationship is not necessarily valid *a priori* for other worlds; even on Earth, the reliability of the euphotic zone as a measure of the photosynthesis zone depth has been questioned (Banse 2004; Marra et al. 2014).

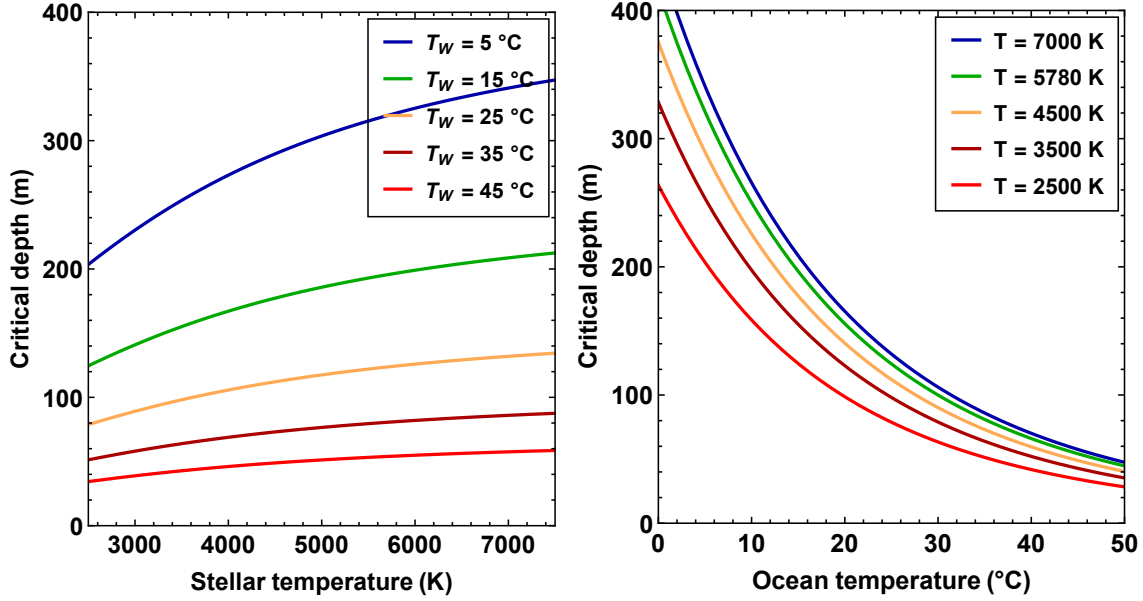


Figure 4. In both panels, the critical depth (Z_{CR}) - the location where the vertically integrated net growth rate is zero - is plotted. Left panel: variation of Z_{CR} with stellar temperature (in K) shown for different ocean temperatures. Right panel: variation of Z_{CR} with ocean temperature (in $^{\circ}\text{C}$) shown for different stellar temperatures.

The NPP will depend not only on the stellar and ocean temperatures but also on inherent biological factors such as C_{sur} that are spatially and temporally very heterogeneous. As the goal of the paper is to construct heuristic global estimates, we rewrite (15) so that it yields the average global value for the Earth at $T = T_{\odot}$ and $T_W = T_0$ (i.e., the parameters for Earth). By adopting the normalization from Field et al. (1998),⁶ we obtain

$$\text{NPP} \approx 1.5 \times 10^{-2} \text{ g C m}^{-2} \text{ h}^{-1} \left(\frac{Z_{CO}^{(R)}}{Z_0} \right) \times \mathcal{P}(T_W) \left(\frac{\mathcal{D}}{0.5} \right) \left(\frac{G(T)}{G(T_{\odot})} \right), \quad (16)$$

where $Z_0 \approx 19$ m represents the compensation depth calculated at the fiducial ocean temperature of T_0 using the methodology in Sec. 3.1, while \mathcal{D} denotes the fraction of time that a given location receives stellar illumination. For planets like Earth, we expect $\mathcal{D} \approx 0.5$ (i.e., equipartition of day and night) whereas tidally locked planets ought to have $\mathcal{D} \approx 1$ on the day side because they receive stellar radiation *in perpetuo*. The auxiliary functions $G(T)$ and $\mathcal{P}(T_W)$ are defined as follows:

$$G(T) = \frac{\mathcal{F}_0}{\mathcal{F}_0 + \mathcal{F}_S}, \quad (17)$$

⁶ Note that subsequent estimates for the oceanic NPP have revised the classic analysis of Field et al. (1998) by $\mathcal{O}(10\%)$ (Westberry et al. 2008), but this has a minimal impact on our subsequent qualitative and quantitative results.

where $\mathcal{F}_S \approx 1.1 \times 10^3 \mu\text{mol m}^{-2} \text{ s}^{-1}$, and the stellar temperature is implicitly present via \mathcal{F}_0 .

$$\mathcal{P}(T_W) = \left[\frac{1 + \exp \left[\frac{E_h}{k_B} \left(\frac{1}{T_h} - \frac{1}{T_0} \right) \right]}{1 + \exp \left[\frac{E_h}{k_B} \left(\frac{1}{T_h} - \frac{1}{T_W} \right) \right]} \right] \times \exp \left[\frac{E_a}{k_B} \left(\frac{1}{T_0} - \frac{1}{T_W} \right) \right], \quad (18)$$

where $E_a \approx 0.74$ eV, $E_h \approx 6.10$ eV and $T_h \approx 34$ $^{\circ}\text{C}$ (Barton et al. 2020, pg. 726). Here, we have constructed (16) and (17) based on Behrenfeld et al. (2005, Section 2.4) and Behrenfeld & Falkowski (1997, Equation 10), but one point of divergence is that we have utilized the SharpeSchoolfield equation as a proxy for $P_{opt}(T_W)$ (Barton et al. 2020) in lieu of Behrenfeld & Falkowski (1997, Equation 11), as the latter becomes invalid for $T_W > 30$ $^{\circ}\text{C}$. The precise expression for $P_{opt}(T_W)$ for phytoplankton has proven challenging to accurately pin down. In consequence, a diverse array of functions, some exhibiting exactly opposite trends with temperature, have been employed for this purpose (Behrenfeld et al. 2005). Hence, we recommend that the ensuing results should be interpreted with due caution.

We have presented the NPP for the two Earth-analogs (Planet G and Planet M) in Table 1. There are several interesting results that emerge from inspecting this table. We begin by considering Planet G, which orbits a solar twin and enables us to gauge the role of T_W . We see that the NPP increases with ocean temperature up to ~ 30 $^{\circ}\text{C}$, but this rise is relatively modest. It is primarily driven by the fact that the rate of carbon fixation, as encapsulated by $\mathcal{P}(T_W)$, increases with temperature in

Table 1. Net primary productivity for the Earth-analogs

Ocean temperature ($^{\circ}\text{C}$)	Relative NPP of Planet G	Relative NPP of Planet M
5	0.4	9×10^{-3}
10	0.6	10^{-2}
15	0.9	10^{-2}
20	1.4	8×10^{-3}
25	2.0	0
30	2.7	0
35	1.2	0
40	6×10^{-2}	0
45	2×10^{-3}	0

Notes: The NPP is expressed in terms of the temporally averaged value associated with modern Earth’s oceans, namely, $1.5 \times 10^{-2} \text{ g C m}^{-2} \text{ h}^{-1}$. The NPP for these two Earth-analogs is calculated by deploying (16). Planet G orbits a solar twin whereas Planet M is situated near a late-type M-dwarf akin to TRAPPIST-1; the other properties of the two planets are otherwise identical.

this regime. Once the peak temperature of the thermal performance curve is attained (T_{pk}), however, the rate of carbon fixation declines sharply, and thereby drives the estimated steep decline in NPP for $T_W > 35^{\circ}\text{C}$.

Now, let us turn our attention to Planet M around a late-type M-dwarf similar to TRAPPIST-1. Even for a fixed temperature, say $T_W = 5^{\circ}\text{C}$, we notice that the NPP is lower than Planet G by roughly two orders of magnitude. The reasons for the diminished NPP are twofold: (i) the compensation depth is much reduced, as already pointed out in Sec. 3.1, and (ii) the flux of PAR is corresponding lower at the surface, thereby making the last term on the right-hand-side of (16) smaller than unity. The next major feature we notice is that the NPP vanishes above $T_W \sim 20^{\circ}\text{C}$. This result is a direct consequence of the fact that the compensation depth becomes zero above a threshold temperature as explained in Sec. 3.1. Hence, exoplanets orbiting late-type M-dwarfs may have a low likelihood of large-scale carbon fixation by phytoplankton-like biota. Of course, the NPP is not guaranteed to become zero *sensu stricto* because anoxygenic photoautotrophs are capable of carbon fixation by definition (Konhauser 2007; Schlesinger & Bernhardt 2013), as are many microbial taxa in the deep biosphere (Orcutt et al. 2011; Edwards et al. 2012).

4. DISCUSSION

We will discuss some of the implications of our work in connection with mapping the trajectories of the Earth as well as M-dwarf exoplanets.

4.1. The past and future Earth

We begin by tackling the ramifications of the preceding analysis for the Earth’s aquatic biosphere, with respect to both its past, present and future.

As noted previously, there is a sharp downswing in NPP shortly after the peak temperature T_{pk} is attained. While there are grounds for contending that $T_{\text{pk}} \sim 30^{\circ}\text{C}$

(Barton et al. 2020), this matter is admittedly not conclusively settled. Now, let us suppose that the Earth’s temperature was raised by $\sim 10^{\circ}\text{C}$ abruptly. In large swathes of the ocean, it is conceivable that $T_W > T_{\text{pk}}$, thereby triggering a sharp downswing in the NPP in these regions. In turn, given that phytoplankton are the foundation of oceanic food webs and trophic interactions (Barnes & Hughes 1999; Valiela 2015; Kirchman 2018), this rapid decline in NPP ought to have adverse consequences for marine ecosystems and could thus potentially drive a mass extinction event.

Recent theoretical modeling and the analysis of oxygen isotope ratios from biogenic apatite indicates that the Paleo-Tethys sea underwent a warming of $\sim 11^{\circ}\text{C}$ due to massive volcanic eruptions (i.e., the Siberian traps) toward the end of the Permian (Penn et al. 2018); see also Sun et al. (2012). It is well-known that the ensuing PermianTriassic extinction event was the largest of its kind in the Phanerozoic, operating over a timescale of $\sim 0.06 \text{ Myr}$ (Burgess et al. 2014), and entailed a recovery time of $\sim 10 \text{ Myr}$ (Chen & Benton 2012). The reasons for the PTr extinction are manifold and still subject to some debate regarding their relative impact (Knoll et al. 2007; Clarkson et al. 2015; Bond & Grasby 2017). Our work lends further credence to the hypothesis that the depth of the photosynthesis zone and NPP were reduced significantly in this period.

Several authors have identified certain similarities between the P-T extinction and the ongoing Anthropocene extinction, and addressed the deleterious effects of global warming on phytoplankton and oceanic NPP (Hoegh-Guldberg & Bruno 2010; Barnosky et al. 2011; Payne & Clapham 2012; Munday et al. 2013; Halsey & Jones 2015; McCauley et al. 2015; Behrenfeld et al. 2016; Penn et al. 2018). As this subject has been extensively investigated, we shall not comment further on it here. It suffices to say that rapidly rising temperatures are eventually anticipated to drive the NPP downwards and

instigate large-scale extinctions of marine biota. There is, however, another subject that has not been as widely studied because it lies in the distant future.

As the Sun continues to grow brighter, the surface temperature will also increase commensurately because of the greenhouse effect until the Earth eventually becomes uninhabitable (Caldeira & Kasting 1992; Goldblatt & Watson 2012; Rushby et al. 2013). Based on Wolf & Toon (2015, Section 3.1), we note that a global temperature of 312 K is expected when the solar luminosity is 1.1 times the present-day value. By utilizing Gough (1981, Equation 1), the stellar luminosity associated with this temperature is expected to occur ~ 1.2 Gyr in the future. It is important to note, however, that climate models do not fully agree on the critical flux at which the greenhouse state is likely to be activated, implying that a timescale of < 1 Gyr ought not be ruled out (Goldblatt et al. 2013; Leconte et al. 2013; Kasting et al. 2015; Popp et al. 2016; Wolf et al. 2017).

If we suppose that the global ocean temperature tracks the average surface temperature, the above analysis suggests that $T_W \sim 39^\circ\text{C}$ would occur ~ 1.2 Gyr hereafter. After examining Table 1, we find that the oceanic NPP at this T_W is likely to be $< 10\%$ of the present-day value. On account of the diminished NPP, eventual depletion of atmospheric O_2 is plausible for reasons adumbrated in the next paragraph, namely, when the sinks outpace the source(s). A decline in atmospheric oxygen could, in turn, led to the extinction of much complex life that requires high O_2 . Thus, *in toto*, the biosphere is unlikely to exhibit the same complexity as that of present-day Earth, which is broadly consistent with earlier predictions by O’Malley-James et al. (2013, 2014).

4.2. *M-dwarf exoplanets*

Now, let us turn our attention to Planet M, the hypothesized exoplanet around a late-type M-dwarf.

We have noted previously that the NPP is only a few percent of the Earth’s current oceanic NPP. Hence, because of the low NPP, unless the burial efficiency of organic carbon is unusually high, it is likely that the flux of O_2 contributed by oxygenic photosynthesis will be correspondingly small. Hence, it becomes more feasible for the sinks of atmospheric O_2 (e.g., continental weathering and volcanic outgassing) to dominate this source. The end result is that O_2 has a low likelihood of accumulating to detectable levels in the atmosphere (Catling & Kasting 2017). This potential development has two consequences in turn. First, O_2 has been conjectured to be a prerequisite for complex life (Knoll 1985; Catling et al. 2005), at least up to a certain limit (Lingam 2020). Hence, the evolution of complex life might be suppressed on this category of worlds. Second, the absence of atmospheric O_2 or O_3 for the aforementioned reasons despite the existence of a biosphere is one example of a “false negative”, which can hinder or complicate the search for extraterrestrial life (Reinhard et al. 2017).

It is instructive to compare our results with prior analyses of similar topics. Wolstencroft & Raven (2002, Table A9) calculated the oceanic NPP, albeit at a fixed depth of 10 m using a simple model based on the photon flux, and found that it is ~ 5 times lower for an Earth-analog around an M0 star. In a similar vein, Lehmer et al. (2018) and Lingam & Loeb (2019e) employed simple models for the NPP linearly proportional to the photon flux and found that late-type M-dwarfs are unlikely to have biospheres with the same NPP as modern Earth and build up atmospheric O_2 to detectable levels. Thus, by and large, our work is compatible with earlier studies, but it took several other environmental and physiological variables into account.

There is a notable caveat that we have implicitly presumed heretofore that merits a brief discussion. Although we have explored the characteristics of aquatic photosynthesis, we have relied upon the photon flux and the ambient temperature as the major input parameters. In actuality, however, the NPP is also dictated by the prevalence of nutrients, especially the ultimate limiting nutrient phosphate (Tyrrell 1999; Filippelli 2008; Schlesinger & Bernhardt 2013; Kipp & Stüeken 2017; Laakso & Schrag 2018, 2019; Hao et al. 2020). Water worlds are ostensibly hampered in this respect due to their potentially lower rates of weathering and nutrient delivery to oceans (Wordsworth & Pierrehumbert 2013; Kite & Ford 2018; Lingam & Loeb 2018c, 2019c; Olson et al. 2020). Hence, such planets around late-type M-dwarfs may be doubly disadvantaged by the paucity of nutrients and photons in the PAR range.

It is helpful to examine the prospects for testing our results at this juncture. A number of publications mentioned in the prior paragraph have already outlined strategies to test whether the stellar spectral type affects the NPP and the accompanying rise in atmospheric O_2 levels. Therefore, we will restrict ourselves to worlds with varying ocean temperature. As Table 1 reveals, a fairly steep decline in the NPP is expected above a certain cutoff temperature. On the other hand, an inspection of (15) suggests that the surface density of chlorophyll (C_{sur}), which is treated like an independent parameter, is not necessarily affected. Hence, at least in principle, the detection of photoautotrophs ought to be feasible via the photosynthetic red edge (Seager et al. 2005), especially if the organisms cover a large fraction of the surface (O’Malley-James & Kaltenegger 2019).

If we can therefore sample enough planets and discern a critical ocean temperature (for which the surface temperature might serve as a rough proxy) above which no biogenic O_2 and O_3 are detected but a tangible photosynthetic red edge is found, such a distinct correlation could provide an avenue for falsifying our hypothesis. However, this strategy is not easily realizable in the near-future because it calls for access to a sufficiently large sample of worlds with reliable biosignatures

and surface temperature measurements (Grenfell 2017; Schwieterman et al. 2018; Fujii et al. 2018).

5. CONCLUSIONS

In this paper, we investigated how the ambient ocean temperature T_W dictates the characteristics of aquatic biospheres on Earth-like worlds, albeit under the key assumption that the putative biota resemble phytoplankton - the chief sources of NPP in Earth's oceans - in terms of their physiological properties.

We began by estimating the compensation depth and critical depth, as they serve to quantify the depths at which the net growth rate and vertically integrated net growth rate become zero, respectively. We showed that the ocean temperature has a relatively moderate influence on the compensation depth for an Earth-analog around a solar twin (Planet G), as Z_{CO} varies only by a factor of < 3 . In contrast, when it comes to an Earth-like world orbiting a late-type M-dwarf (Planet M) akin to TRAPPIST-1, we found that T_W causes Z_{CO} to vary by at least an order of magnitude. Furthermore, sufficiently warm oceans may preclude phytoplankton-like biota from existing on these worlds altogether. We calculated the critical depth and showed that it is sensitive to T_W , and varies by nearly an order of magnitude for the temperature range considered herein.

Next, we examined the NPP in the oceans of Planet G and Planet M as a function of the ocean temperature. The reason for studying the NPP is discussed in more detail below. This calculation entailed the estimation of several variables, but a few of them have not been robustly expressed as functions of T_W . Bearing this caveat in mind, we found that the NPP on Planet G was not very sensitive to T_W until it exceeded a certain threshold after which the rate of carbon fixation dropped precip-

itously and drove a corresponding decline in the NPP. For the case of Planet M, the NPP was determined to be $\lesssim 1\%$ that of modern Earth, primarily due to the shallowness of the photosynthesis zone as well as the lower PAR fluxes. When ocean temperatures were sufficiently raised, the conditions for phytoplankton-like biota became untenable as noted in the earlier paragraph, and consequently led to the NPP approaching zero.

Lastly, we analyzed the ramifications of our work in relation to Earth and exoplanets from late-type M-dwarfs. We discussed how an increase of $\sim 10^\circ\text{C}$ in the ocean temperature - such as what probably occurred during the P-Tr extinction due to volcanism and is expected to happen $\lesssim 1$ Gyr in the future because of the increasing solar luminosity - could radically transform Earth's aquatic biosphere and make its NPP $< 10\%$ of its present-day value in certain regions of the oceans. In a similar vein, we pointed out that the aquatic biospheres of Earth-like worlds around late-type M-dwarfs may have NPPs that are $\lesssim 1\%$ of Earth's current oceanic NPP. If this prediction is correct, these worlds would be unlikely to accumulate atmospheric O_2 , but signatures of life are potentially detectable by means of the photosynthetic red edge. We concluded our discussion by sketching methods by which the behavior of NPP with temperature might be gauged by future observations.

ACKNOWLEDGMENTS

This research was supported in part by the Breakthrough Prize Foundation, Harvard University's Faculty of Arts and Sciences, and the Institute for Theory and Computation (ITC) at Harvard University.

REFERENCES

- Angilletta, M. J. 2009, *Thermal Adaptation: A Theoretical and Empirical Synthesis* (Oxford Univ. Press)
- Arndt, N. T., & Nisbet, E. G. 2012, *Annu. Rev. Earth Planet. Sci.*, 40, 521, doi: [10.1146/annurev-earth-042711-105316](https://doi.org/10.1146/annurev-earth-042711-105316)
- Bambach, R. K. 2006, *Annu. Rev. Earth Planet. Sci.*, 34, 127, doi: [10.1146/annurev.earth.33.092203.122654](https://doi.org/10.1146/annurev.earth.33.092203.122654)
- Banse, K. 2004, *Limnol. Oceanogr. Bull.*, 13, 49, doi: [10.1002/lob.200413349](https://doi.org/10.1002/lob.200413349)
- Bar-On, Y. M., Phillips, R., & Milo, R. 2018, *Proc. Natl. Acad. Sci. USA*, 115, 6506, doi: [10.1073/pnas.1711842115](https://doi.org/10.1073/pnas.1711842115)
- Barnes, R. S. K., & Hughes, R. N. 1999, *An Introduction to Marine Ecology*, 3rd edn. (Blackwell Publishing)
- Barnosky, A. D., Matzke, N., Tomiya, S., et al. 2011, *Nature*, 471, 51, doi: [10.1038/nature09678](https://doi.org/10.1038/nature09678)
- Barton, S., Jenkins, J., Buckling, A., et al. 2020, *Ecol. Lett.*, 23, 722, doi: [10.1111/ele.13469](https://doi.org/10.1111/ele.13469)
- Behrenfeld, M. J. 2010, *Ecology*, 91, 977, doi: [10.1890/09-1207.1](https://doi.org/10.1890/09-1207.1)
- Behrenfeld, M. J., Boss, E., Siegel, D. A., & Shea, D. M. 2005, *Global Biogeochem. Cy.*, 19, GB1006, doi: [10.1029/2004GB002299](https://doi.org/10.1029/2004GB002299)
- Behrenfeld, M. J., & Falkowski, P. G. 1997, *Limnol. Oceanogr.*, 42, 1, doi: [10.4319/lo.1997.42.1.0001](https://doi.org/10.4319/lo.1997.42.1.0001)
- Behrenfeld, M. J., O'Malley, R. T., Boss, E. S., et al. 2016, *Nat. Clim. Change*, 6, 323, doi: [10.1038/nclimate2838](https://doi.org/10.1038/nclimate2838)
- Berg, I. A. 2011, *Appl. Environ. Microbiol.*, 77, 1925, doi: [10.1128/AEM.02473-10](https://doi.org/10.1128/AEM.02473-10)
- Blankenship, R. E. 2014, *Molecular Mechanisms of Photosynthesis*, 2nd edn. (Wiley-Blackwell)

- Blois, J. L., Zarnetske, P. L., Fitzpatrick, M. C., & Finnegan, S. 2013, *Science*, 341, 499, doi: [10.1126/science.1237184](https://doi.org/10.1126/science.1237184)
- Bond, D. P. G., & Grasby, S. E. 2017, *Palaeogeogr. Palaeoclimatol. Palaeoecol.*, 478, 3, doi: [10.1016/j.palaeo.2016.11.005](https://doi.org/10.1016/j.palaeo.2016.11.005)
- Brown, J. H., Gillooly, J. F., Allen, A. P., Savage, V. M., & West, G. B. 2004, *Ecology*, 85, 1771, doi: [10.1890/03-9000](https://doi.org/10.1890/03-9000)
- Burgess, S. D., Bowring, S., & Shen, S.-z. 2014, *Proc. Natl. Acad. Sci. USA*, 111, 3316, doi: [10.1073/pnas.1317692111](https://doi.org/10.1073/pnas.1317692111)
- Caldeira, K., & Kasting, J. F. 1992, *Nature*, 360, 721, doi: [10.1038/360721a0](https://doi.org/10.1038/360721a0)
- Canfield, D., Kristensen, E., & Thamdrup, B. 2005, *Aquatic Geomicrobiology, Advances in Marine Biology* No. 48 (Elsevier)
- Catling, D. C., Glein, C. R., Zahnle, K. J., & McKay, C. P. 2005, *Astrobiology*, 5, 415, doi: [10.1089/ast.2005.5.415](https://doi.org/10.1089/ast.2005.5.415)
- Catling, D. C., & Kasting, J. F. 2017, *Atmospheric Evolution on Inhabited and Lifeless Worlds* (Cambridge University Press)
- Checlair, J. H., Olson, S. L., Jansen, M. F., & Abbot, D. S. 2019, *Astrophys. J. Lett.*, 884, L46, doi: [10.3847/2041-8213/ab487d](https://doi.org/10.3847/2041-8213/ab487d)
- Chen, J., & Kipping, D. 2017, *Astrophys. J.*, 834, 17, doi: [10.3847/1538-4357/834/1/17](https://doi.org/10.3847/1538-4357/834/1/17)
- Chen, M., & Blankenship, R. E. 2011, *Trends Plant Sci.*, 16, 427, doi: [10.1016/j.tplants.2011.03.011](https://doi.org/10.1016/j.tplants.2011.03.011)
- Chen, Z.-Q., & Benton, M. J. 2012, *Nat. Geosci.*, 5, 375, doi: [10.1038/ngeo1475](https://doi.org/10.1038/ngeo1475)
- Chiswell, S. 2011, *Mar. Ecol. Prog. Ser.*, 443, 39, doi: [10.3354/meps09453](https://doi.org/10.3354/meps09453)
- Chyba, C. F., & Hand, K. P. 2001, *Science*, 292, 2026, doi: [10.1126/science.1060081](https://doi.org/10.1126/science.1060081)
- Clarke, A. 2014, *Int. J. Astrobiol.*, 13, 141, doi: [10.1017/S1473550413000438](https://doi.org/10.1017/S1473550413000438)
- Clarke, A. 2017, *Principles of Thermal Ecology: Temperature, Energy and Life* (Oxford University Press)
- Clarkson, M. O., Kasemann, S. A., Wood, R. A., et al. 2015, *Science*, 348, 229, doi: [10.1126/science.aaa0193](https://doi.org/10.1126/science.aaa0193)
- Cockell, C. S., Bush, T., Bryce, C., et al. 2016, *Astrobiology*, 16, 89, doi: [10.1089/ast.2015.1295](https://doi.org/10.1089/ast.2015.1295)
- Corkrey, R., McMeekin, T. A., Bowman, J. P., Olley, J., & Ratkowsky, D. 2018, *Int. J. Astrobiol.*, 17, 17, doi: [10.1017/S1473550416000501](https://doi.org/10.1017/S1473550416000501)
- Cossins, A. R., & Bowler, K. 1987, *Temperature Biology of Animals* (Chapman & Hall)
- Cowan, N. B., & Abbot, D. S. 2014, *Astrophys. J.*, 781, 27, doi: [10.1088/0004-637X/781/1/27](https://doi.org/10.1088/0004-637X/781/1/27)
- Cullum, J., & Stevens, D. P. 2016, *Proc. Natl. Acad. Sci. USA*, 113, 4278, doi: [10.1073/pnas.1522034113](https://doi.org/10.1073/pnas.1522034113)
- Deamer, D., & Weber, A. L. 2010, *Cold Spring Harb. Perspect. Biol.*, 2, a004929, doi: [10.1101/cshperspect.a004929](https://doi.org/10.1101/cshperspect.a004929)
- Del Genio, A. D., Way, M. J., Kiang, N. Y., et al. 2019, *Astrophys. J.*, 887, 197, doi: [10.3847/1538-4357/ab57fd](https://doi.org/10.3847/1538-4357/ab57fd)
- Delrez, L., Gillon, M., Triaud, A. H. M. J., et al. 2018, *Mon. Not. R. Astron. Soc.*, 475, 3577, doi: [10.1093/mnras/sty051](https://doi.org/10.1093/mnras/sty051)
- Dole, S. H. 1964, *Habitable planets for man* (Blaisdell Pub. Co.)
- Dorn, C., Mosegaard, K., Grimm, S. L., & Alibert, Y. 2018, *Astrophys. J.*, 865, 20, doi: [10.3847/1538-4357/aad95d](https://doi.org/10.3847/1538-4357/aad95d)
- Edwards, K. J., Becker, K., & Colwell, F. 2012, *Annu. Rev. Earth Planet. Sci.*, 40, 551, doi: [10.1146/annurev-earth-042711-105500](https://doi.org/10.1146/annurev-earth-042711-105500)
- Ehlmann, B. L., Anderson, F. S., Andrews-Hanna, J., et al. 2016, *J. Geophys. Res. Planets*, 121, 1927, doi: [10.1002/2016JE005134](https://doi.org/10.1002/2016JE005134)
- Falkowski, P. G., Katz, M. E., Knoll, A. H., et al. 2004, *Science*, 305, 354, doi: [10.1126/science.1095964](https://doi.org/10.1126/science.1095964)
- Falkowski, P. G., & Raven, J. A. 2007, *Aquatic photosynthesis*, 2nd edn. (Princeton University Press)
- Field, C. B., Behrenfeld, M. J., Randerson, J. T., & Falkowski, P. 1998, *Science*, 281, 237, doi: [10.1126/science.281.5374.237](https://doi.org/10.1126/science.281.5374.237)
- Filippelli, G. M. 2008, *Elements*, 4, 89, doi: [10.2113/GSELEMENTS.4.2.89](https://doi.org/10.2113/GSELEMENTS.4.2.89)
- Fischer, A. D., Moberg, E. A., Alexander, H., et al. 2014, *Oceanography*, 27, 222, doi: [0.5670/oceanog.2014.26](https://doi.org/0.5670/oceanog.2014.26)
- Flament, N., Coltice, N., & Rey, P. F. 2008, *Earth Planet. Sci. Lett.*, 275, 326, doi: [10.1016/j.epsl.2008.08.029](https://doi.org/10.1016/j.epsl.2008.08.029)
- Fujii, Y., Angerhausen, D., Deitrick, R., et al. 2018, *Astrobiology*, 18, 739, doi: [10.1089/ast.2017.1733](https://doi.org/10.1089/ast.2017.1733)
- Gillon, M., Triaud, A. H. M. J., Demory, B.-O., et al. 2017, *Nature*, 542, 456, doi: [10.1038/nature21360](https://doi.org/10.1038/nature21360)
- Gillooly, J. F., Brown, J. H., West, G. B., Savage, V. M., & Charnov, E. L. 2001, *Science*, 293, 2248, doi: [10.1126/science.1061967](https://doi.org/10.1126/science.1061967)
- Goldblatt, C. 2015, *Astrobiology*, 15, 362, doi: [10.1089/ast.2014.1268](https://doi.org/10.1089/ast.2014.1268)
- Goldblatt, C., Robinson, T. D., Zahnle, K. J., & Crisp, D. 2013, *Nat. Geosci.*, 6, 661, doi: [10.1038/ngeo1892](https://doi.org/10.1038/ngeo1892)
- Goldblatt, C., & Watson, A. J. 2012, *Philos. Trans. Royal Soc. A*, 370, 4197, doi: [10.1098/rsta.2012.0004](https://doi.org/10.1098/rsta.2012.0004)
- Gough, D. O. 1981, *Sol. Phys.*, 74, 21, doi: [10.1007/BF00151270](https://doi.org/10.1007/BF00151270)
- Gran, H. H., & Braarud, T. 1935, *J. Biol. Bd Can.*, 1, 279, doi: [10.1139/f35-012](https://doi.org/10.1139/f35-012)
- Grenfell, J. L. 2017, *Phys. Rep.*, 713, 1, doi: [10.1016/j.physrep.2017.08.003](https://doi.org/10.1016/j.physrep.2017.08.003)

- Grimm, S. L., Demory, B.-O., Gillon, M., et al. 2018, *Astron. Astrophys.*, 613, A68, doi: [10.1051/0004-6361/201732233](https://doi.org/10.1051/0004-6361/201732233)
- Hale, G. M., & Querry, M. R. 1973, *Appl. Opt.*, 12, 555, doi: [10.1364/AO.12.000555](https://doi.org/10.1364/AO.12.000555)
- Hallam, A., & Wignall, P. B. 1997, *Mass Extinctions and Their Aftermath* (Oxford University Press)
- Halsey, K. H., & Jones, B. M. 2015, *Annu. Rev. Mar. Sci.*, 7, 265, doi: [10.1146/annurev-marine-010814-015813](https://doi.org/10.1146/annurev-marine-010814-015813)
- Hao, J., Knoll, A. H., Huang, F., et al. 2020, *Geochim. Cosmochim. Acta*, doi: [10.1016/j.gca.2020.04.005](https://doi.org/10.1016/j.gca.2020.04.005)
- Hart, M. H. 1979, *Icarus*, 37, 351, doi: [10.1016/0019-1035\(79\)90141-6](https://doi.org/10.1016/0019-1035(79)90141-6)
- Heller, R., & Armstrong, J. 2014, *Astrobiology*, 14, 50, doi: [10.1089/ast.2013.1088](https://doi.org/10.1089/ast.2013.1088)
- Hochachka, P. W., & Somero, G. N. 2002, *Biochemical Adaptation: Mechanism and Process in Physiological Evolution* (Oxford University Press)
- Hoegh-Guldberg, O., & Bruno, J. F. 2010, *Science*, 328, 1523, doi: [10.1126/science.1189930](https://doi.org/10.1126/science.1189930)
- Hu, Y., & Yang, J. 2014, *Proc. Natl. Acad. Sci. USA*, 111, 629, doi: [10.1073/pnas.1315215111](https://doi.org/10.1073/pnas.1315215111)
- Iizuka, T., Komiya, T., Rino, S., Maruyama, S., & Hirata, T. 2010, *Geochim. Cosmochim. Acta*, 74, 2450, doi: [10.1016/j.gca.2010.01.023](https://doi.org/10.1016/j.gca.2010.01.023)
- Jin, S., & Mordasini, C. 2018, *Astrophys. J.*, 853, 163, doi: [10.3847/1538-4357/aa9f1e](https://doi.org/10.3847/1538-4357/aa9f1e)
- Johnson, B. W., & Wing, B. A. 2020, *Nat. Geosci.*, 13, 243, doi: [10.1038/s41561-020-0538-9](https://doi.org/10.1038/s41561-020-0538-9)
- Judson, O. P. 2017, *Nat. Ecol. Evol.*, 1, 0138, doi: [10.1038/s41559-017-0138](https://doi.org/10.1038/s41559-017-0138)
- Kane, S. R., Arney, G., Crisp, D., et al. 2019, *J. Geophys. Res. Planets*, 124, 2015, doi: [10.1029/2019JE005939](https://doi.org/10.1029/2019JE005939)
- Kasting, J. 2012, *How to Find a Habitable Planet* (Princeton University Press)
- Kasting, J. F., Chen, H., & Kopparapu, R. K. 2015, *Astrophys. J. Lett.*, 813, L3, doi: [10.1088/2041-8205/813/1/L3](https://doi.org/10.1088/2041-8205/813/1/L3)
- Kasting, J. F., Whitmire, D. P., & Reynolds, R. T. 1993, *Icarus*, 101, 108, doi: [10.1006/icar.1993.1010](https://doi.org/10.1006/icar.1993.1010)
- Kiang, N. Y., Segura, A., Tinetti, G., et al. 2007, *Astrobiology*, 7, 252, doi: [10.1089/ast.2006.0108](https://doi.org/10.1089/ast.2006.0108)
- Kingsolver, J. G. 2009, *Am. Nat.*, 174, 755, doi: [10.1086/648310](https://doi.org/10.1086/648310)
- Kipp, M. A., & Stüeken, E. E. 2017, *Sci. Adv.*, 3, eaao4795, doi: [10.1126/sciadv.aao4795](https://doi.org/10.1126/sciadv.aao4795)
- Kirchman, D. L. 2018, *Processes in Microbial Ecology*, 2nd edn. (Oxford University Press)
- Kirk, J. T. O. 2011, *Light and Photosynthesis in Aquatic Ecosystems*, 3rd edn. (Cambridge University Press)
- Kite, E. S., & Ford, E. B. 2018, *Astrophys. J.*, 864, 75, doi: [10.3847/1538-4357/aad6e0](https://doi.org/10.3847/1538-4357/aad6e0)
- Knoll, A. H. 1985, in *IAU Symposium*, Vol. 112, *The Search for Extraterrestrial Life: Recent Developments*, ed. M. D. Papagiannis, 201–211, doi: [10.1017/S0074180900146534](https://doi.org/10.1017/S0074180900146534)
- Knoll, A. H. 2015, *Life on a Young Planet: The First Three Billion Years of Evolution on Earth*, Princeton Science Library (Princeton University Press)
- Knoll, A. H., Bambach, R. K., Payne, J. L., Pruss, S., & Fischer, W. W. 2007, *Earth Planet. Sci. Lett.*, 256, 295, doi: [10.1016/j.epsl.2007.02.018](https://doi.org/10.1016/j.epsl.2007.02.018)
- Kolbert, E. 2014, *The Sixth Extinction: An Unnatural History* (Bloomsbury)
- Konhauser, K. O. 2007, *Introduction to Geomicrobiology* (Blackwell Publishing)
- Kopparapu, R. K., Ramirez, R., Kasting, J. F., et al. 2013, *Astrophys. J.*, 765, 131, doi: [10.1088/0004-637X/765/2/131](https://doi.org/10.1088/0004-637X/765/2/131)
- Kou, L., Labrie, D., & Chylek, P. 1993, *Appl. Opt.*, 32, 3531, doi: [10.1364/AO.32.003531](https://doi.org/10.1364/AO.32.003531)
- Kuchner, M. J. 2003, *Astrophys. J. Lett.*, 596, L105, doi: [10.1086/378397](https://doi.org/10.1086/378397)
- Laakso, T. A., & Schrag, D. P. 2018, *Global Biogeochem. Cy.*, 32, 486, doi: [10.1002/2017GB005832](https://doi.org/10.1002/2017GB005832)
- . 2019, *Geobiology*, 17, 161, doi: [10.1111/gbi.12323](https://doi.org/10.1111/gbi.12323)
- Lane, N. 2002, *Oxygen: the molecule that made the world* (Oxford University Press)
- Langford, V. S., McKinley, A. J., & Quickenden, T. I. 2001, *J. Phys. Chem. A*, 105, 8916, doi: [10.1021/jp010093m](https://doi.org/10.1021/jp010093m)
- Leconte, J., Forget, F., Charnay, B., Wordsworth, R., & Pottier, A. 2013, *Nature*, 504, 268, doi: [10.1038/nature12827](https://doi.org/10.1038/nature12827)
- Lee, Z., Weidemann, A., Kindle, J., et al. 2007, *J. Geophys. Res. Oceans*, 112, C03009, doi: [10.1029/2006JC003802](https://doi.org/10.1029/2006JC003802)
- Léger, A., Selsis, F., Sotin, C., et al. 2004, *Icarus*, 169, 499, doi: [10.1016/j.icarus.2004.01.001](https://doi.org/10.1016/j.icarus.2004.01.001)
- Lehmer, O. R., Catling, D. C., Parenteau, M. N., & Hoehler, T. M. 2018, *Astrophys. J.*, 859, 171, doi: [10.3847/1538-4357/aac1d4](https://doi.org/10.3847/1538-4357/aac1d4)
- Lingam, M. 2020, *Astron. J.*, 159, 144, doi: [10.3847/1538-3881/ab737f](https://doi.org/10.3847/1538-3881/ab737f)
- Lingam, M., & Loeb, A. 2018a, *Astrobiology*, 18, 967, doi: [10.1089/ast.2017.1718](https://doi.org/10.1089/ast.2017.1718)
- . 2018b, *Astrophys. J. Lett.*, 857, L17, doi: [10.3847/2041-8213/aabd86](https://doi.org/10.3847/2041-8213/aabd86)
- . 2018c, *Astron. J.*, 156, 151, doi: [10.3847/1538-3881/aada02](https://doi.org/10.3847/1538-3881/aada02)
- . 2019a, *Rev. Mod. Phys.*, 91, 021002, doi: [10.1103/RevModPhys.91.021002](https://doi.org/10.1103/RevModPhys.91.021002)

- . 2019b, *Astrophys. J.*, 883, 143, doi: [10.3847/1538-4357/ab3f35](https://doi.org/10.3847/1538-4357/ab3f35)
- . 2019c, *Astron. J.*, 157, 25, doi: [10.3847/1538-3881/aaf420](https://doi.org/10.3847/1538-3881/aaf420)
- . 2019d, *Int. J. Astrobiol.*, 18, 112, doi: [10.1017/S1473550418000083](https://doi.org/10.1017/S1473550418000083)
- . 2019e, *Mon. Not. R. Astron. Soc.*, 485, 5924, doi: [10.1093/mnras/stz847](https://doi.org/10.1093/mnras/stz847)
- . 2020, *Astrophys. J. Lett.*, 889, L15, doi: [10.3847/2041-8213/ab6a14](https://doi.org/10.3847/2041-8213/ab6a14)
- Litjens, R. A., Quickenden, T. I., & Freeman, C. G. 1999, *Appl. Opt.*, 38, 1216, doi: [10.1364/AO.38.001216](https://doi.org/10.1364/AO.38.001216)
- Lunine, J. I. 2013, *Earth: Evolution of a Habitable World*, 2nd edn. (Cambridge University Press)
- Mann, K. H., & Lazier, J. R. N. 2006, *Dynamics of Marine Ecosystems: Biological-Physical Interactions in the Oceans*, 3rd edn. (Blackwell Publishing)
- Marra, J. 2004, *Geophys. Res. Lett.*, 31, L06305, doi: [10.1029/2003GL018881](https://doi.org/10.1029/2003GL018881)
- Marra, J. F., Lance, V. P., Vaillancourt, R. D., & Hargreaves, B. R. 2014, *Deep Sea Res. Part I Oceanogr. Res.*, 83, 45, doi: [10.1016/j.dsr.2013.09.005](https://doi.org/10.1016/j.dsr.2013.09.005)
- Marshall, S. M., & Orr, A. P. 1928, *J. Mar. Biol. Ass. U. K.*, 15, 321, doi: [10.1017/S0025315400055703](https://doi.org/10.1017/S0025315400055703)
- McCauley, D. J., Pinsky, M. L., Palumbi, S. R., et al. 2015, *Science*, 347, 1255641, doi: [10.1126/science.1255641](https://doi.org/10.1126/science.1255641)
- McKay, C. P. 2014, *Proc. Natl. Acad. Sci. USA*, 111, 12628, doi: [10.1073/pnas.1304212111](https://doi.org/10.1073/pnas.1304212111)
- Merino, N., Aronson, H. S., Bojanova, D. P., et al. 2019, *Front. Microbiol.*, 10, 780, doi: [10.3389/fmicb.2019.00780](https://doi.org/10.3389/fmicb.2019.00780)
- Middelburg, J. J. 2019, *Marine Carbon Biogeochemistry: A Primer for Earth System Scientists*, SpringerBriefs in Earth System Sciences (Springer), doi: [10.1007/978-3-030-10822-9](https://doi.org/10.1007/978-3-030-10822-9)
- Munday, P. L., Warner, R. R., Monro, K., Pandolfi, J. M., & Marshall, D. J. 2013, *Ecol. Lett.*, 16, 1488, doi: [10.1111/ele.12185](https://doi.org/10.1111/ele.12185)
- Murante, G., Provenzale, A., Vladilo, G., et al. 2020, *Mon. Not. R. Astron. Soc.*, 492, 2638, doi: [10.1093/mnras/stz3529](https://doi.org/10.1093/mnras/stz3529)
- Nelson, D. M., & Smith, W. O. 1991, *Limnol. Oceanogr.*, 36, 1650, doi: [10.4319/lo.1991.36.8.1650](https://doi.org/10.4319/lo.1991.36.8.1650)
- Noack, L., Snellen, I., & Rauer, H. 2017, *Space Sci. Rev.*, 212, 877, doi: [10.1007/s11214-017-0413-1](https://doi.org/10.1007/s11214-017-0413-1)
- Nürnberg, D. J., Morton, J., Santabarbara, S., et al. 2018, *Science*, 360, 1210, doi: [10.1126/science.aar8313](https://doi.org/10.1126/science.aar8313)
- Obata, A., Ishizaka, J., & Endoh, M. 1996, *J. Geophys. Res.*, 101, 20,657, doi: [10.1029/96JC01734](https://doi.org/10.1029/96JC01734)
- Olson, S. L., Jansen, M., & Abbot, D. S. 2020, *Astrophys. J.*, 895, 19, doi: [10.3847/1538-4357/ab88c9](https://doi.org/10.3847/1538-4357/ab88c9)
- O'Malley-James, J. T., Cockell, C. S., Greaves, J. S., & Raven, J. A. 2014, *Int. J. Astrobiol.*, 13, 229, doi: [10.1017/S1473550413000426](https://doi.org/10.1017/S1473550413000426)
- O'Malley-James, J. T., Greaves, J. S., Raven, J. A., & Cockell, C. S. 2013, *Int. J. Astrobiol.*, 12, 99, doi: [10.1017/S147355041200047X](https://doi.org/10.1017/S147355041200047X)
- O'Malley-James, J. T., & Kaltenegger, L. 2019, *Astrophys. J. Lett.*, 879, L20, doi: [10.3847/2041-8213/ab2769](https://doi.org/10.3847/2041-8213/ab2769)
- Orcutt, B. N., Sylvan, J. B., Knab, N. J., & Edwards, K. J. 2011, *Microbiol. Mol. Biol. Rev.*, 75, 361, doi: [10.1128/MMBR.00039-10](https://doi.org/10.1128/MMBR.00039-10)
- Pacifici, M., Foden, W. B., Visconti, P., et al. 2015, *Nat. Clim. Change*, 5, 215, doi: [10.1038/nclimate2448](https://doi.org/10.1038/nclimate2448)
- Pawlowicz, R. 2013, *Nat. Education Knowledge*, 4, 13, doi: [10.1364/AO.32.003531](https://doi.org/10.1364/AO.32.003531)
- Payne, J. L., & Clapham, M. E. 2012, *Annu. Rev. Earth Planet. Sci.*, 40, 89, doi: [10.1146/annurev-earth-042711-105329](https://doi.org/10.1146/annurev-earth-042711-105329)
- Penn, J. L., Deutsch, C., Payne, J. L., & Sperling, E. A. 2018, *Science*, 362, eaat1327, doi: [10.1126/science.aat1327](https://doi.org/10.1126/science.aat1327)
- Pope, R. M., & Fry, E. S. 1997, *Appl. Opt.*, 36, 8710, doi: [10.1364/AO.36.008710](https://doi.org/10.1364/AO.36.008710)
- Popp, M., Schmidt, H., & Marotzke, J. 2016, *Nat. Commun.*, 7, 10627, doi: [10.1038/ncomms10627](https://doi.org/10.1038/ncomms10627)
- Ramirez, R. M. 2018, *Geosciences*, 8, 280, doi: [10.3390/geosciences8080280](https://doi.org/10.3390/geosciences8080280)
- . 2020, *Sci. Rep.*, 10, 7432, doi: [10.1038/s41598-020-64436-z](https://doi.org/10.1038/s41598-020-64436-z)
- Ramirez, R. M., & Levi, A. 2018, *Mon. Not. R. Astron. Soc.*, 477, 4627, doi: [10.1093/mnras/sty761](https://doi.org/10.1093/mnras/sty761)
- Raven, J. A. 2009, *Aquat. Microb. Ecol.*, 56, 177, doi: [10.3354/ame01315](https://doi.org/10.3354/ame01315)
- Regaudie-De-Gioux, A., & Duarte, C. M. 2010, *Global Biogeochem. Cy.*, 24, GB4013, doi: [10.1029/2009GB003639](https://doi.org/10.1029/2009GB003639)
- . 2012, *Global Biogeochem. Cy.*, 26, GB1015, doi: [10.1029/2010GB003907](https://doi.org/10.1029/2010GB003907)
- Reinhard, C. T., Olson, S. L., Schwieterman, E. W., & Lyons, T. W. 2017, *Astrobiology*, 17, 287, doi: [10.1089/ast.2016.1598](https://doi.org/10.1089/ast.2016.1598)
- Ritchie, R. J., Larkum, A. W. D., & Ribas, I. 2018, *Int. J. Astrobiol.*, 17, 147, doi: [10.1017/S1473550417000167](https://doi.org/10.1017/S1473550417000167)
- Rogers, L. A. 2015, *Astrophys. J.*, 801, 41, doi: [10.1088/0004-637X/801/1/41](https://doi.org/10.1088/0004-637X/801/1/41)
- Rothschild, L. J., & Mancinelli, R. L. 2001, *Nature*, 409, 1092, doi: [10.1038/35059215](https://doi.org/10.1038/35059215)
- Röttgers, R., McKee, D., & Utschig, C. 2014, *Opt. Express*, 22, 25093, doi: [10.1364/OE.22.025093](https://doi.org/10.1364/OE.22.025093)
- Rushby, A. J., Claire, M. W., Osborn, H., & Watson, A. J. 2013, *Astrobiology*, 13, 833, doi: [10.1089/ast.2012.0938](https://doi.org/10.1089/ast.2012.0938)

- Salazar, A. M., Olson, S. L., Komacek, T. D., Stephens, H., & Abbot, D. S. 2020, *Astrophys. J. Lett.*, arXiv:2005.14185. <https://arxiv.org/abs/2005.14185>
- Sarmiento, J. L., & Gruber, N. 2006, *Ocean Biogeochemical Dynamics* (Princeton University Press)
- Sathyendranath, S., Ji, R., & Browman, H. I. 2015, *ICES J. Mar. Sci.*, 72, 1892, doi: [10.1093/icesjms/fsv110](https://doi.org/10.1093/icesjms/fsv110)
- Scalo, J., Kaltenegger, L., Segura, A. G., et al. 2007, *Astrobiology*, 7, 85, doi: [10.1089/ast.2006.0125](https://doi.org/10.1089/ast.2006.0125)
- Schlesinger, W. H., & Bernhardt, E. S. 2013, *Biogeochemistry: An Analysis of Global Change*, 3rd edn. (Academic Press)
- Schulte, P. M. 2015, *J. Exp. Biol.*, 218, 1856, doi: [10.1242/jeb.118851](https://doi.org/10.1242/jeb.118851)
- Schwieterman, E. W., Reinhard, C. T., Olson, S. L., Harman, C. E., & Lyons, T. W. 2019, *Astrophys. J.*, 878, 19, doi: [10.3847/1538-4357/ab1d52](https://doi.org/10.3847/1538-4357/ab1d52)
- Schwieterman, E. W., Kiang, N. Y., Parenteau, M. N., et al. 2018, *Astrobiology*, 18, 663, doi: [10.1089/ast.2017.1729](https://doi.org/10.1089/ast.2017.1729)
- Seager, S., Turner, E. L., Schafer, J., & Ford, E. B. 2005, *Astrobiology*, 5, 372, doi: [10.1089/ast.2005.5.372](https://doi.org/10.1089/ast.2005.5.372)
- Shields, A. L., Ballard, S., & Johnson, J. A. 2016, *Phys. Rep.*, 663, 1, doi: [10.1016/j.physrep.2016.10.003](https://doi.org/10.1016/j.physrep.2016.10.003)
- Siegel, D. A., Doney, S. C., & Yoder, J. A. 2002, *Science*, 296, 730, doi: [10.1126/science.1069174](https://doi.org/10.1126/science.1069174)
- Silva, L., Vladilo, G., Schulte, P. M., Murante, G., & Provenzale, A. 2017, *Int. J. Astrobiol.*, 16, 244, doi: [10.1017/S1473550416000215](https://doi.org/10.1017/S1473550416000215)
- Smetacek, V., & Passow, U. 1990, *Limnol. Oceanogr.*, 35, 228, doi: [10.4319/lo.1990.35.1.0228](https://doi.org/10.4319/lo.1990.35.1.0228)
- Stüeken, E. E., Som, S. M., Claire, M., et al. 2020, *Space Sci. Rev.*, 216, 31, doi: [10.1007/s11214-020-00652-3](https://doi.org/10.1007/s11214-020-00652-3)
- Sullivan, J. M., Twardowski, M. S., Zaneveld, J. R. V., et al. 2006, *Appl. Opt.*, 45, 5294, doi: [10.1364/AO.45.005294](https://doi.org/10.1364/AO.45.005294)
- Sun, Y., Joachimski, M. M., Wignall, P. B., et al. 2012, *Science*, 338, 366, doi: [10.1126/science.1224126](https://doi.org/10.1126/science.1224126)
- Sverdrup, H. U. 1953, *J. Cons. Perm. Int. Explor. Mer.*, 18, 287, doi: [10.1093/icesjms/18.3.287](https://doi.org/10.1093/icesjms/18.3.287)
- Sverdrup, H. U., Johnson, M. W., & Fleming, R. H. 1942, *The Oceans: Their Physics, Chemistry, and General Biology* (Prentice-Hall)
- Tarter, J. C., Backus, P. R., Mancinelli, R. L., et al. 2007, *Astrobiology*, 7, 30, doi: [10.1089/ast.2006.0124](https://doi.org/10.1089/ast.2006.0124)
- Tyrrell, T. 1999, *Nature*, 400, 525, doi: [10.1038/22941](https://doi.org/10.1038/22941)
- Unterborn, C. T., Hinkel, N. R., & Desch, S. J. 2018, *Res. Notes AAS*, 2, 116, doi: [10.3847/2515-5172/aacf43](https://doi.org/10.3847/2515-5172/aacf43)
- Valiela, I. 2015, *Marine Ecological Processes*, 3rd edn. (Springer), doi: [10.1007/978-0-387-79070-1](https://doi.org/10.1007/978-0-387-79070-1)
- Ward, L. M., Rasmussen, B., & Fischer, W. W. 2019, *J. Geophys. Res. Biogeosci.*, 124, 211, doi: [10.1029/2018JG004679](https://doi.org/10.1029/2018JG004679)
- Westberry, T., Behrenfeld, M. J., Siegel, D. A., & Boss, E. 2008, *Global Biogeochem. Cy.*, 22, GB2024, doi: [10.1029/2007GB003078](https://doi.org/10.1029/2007GB003078)
- Wolf, E. T., Shields, A. L., Kopparapu, R. K., Haqq-Misra, J., & Toon, O. B. 2017, *Astrophys. J.*, 837, 107, doi: [10.3847/1538-4357/aa5ffc](https://doi.org/10.3847/1538-4357/aa5ffc)
- Wolf, E. T., & Toon, O. B. 2015, *J. Geophys. Res. D*, 120, 5775, doi: [10.1002/2015JD023302](https://doi.org/10.1002/2015JD023302)
- Wolfgang, A., & Lopez, E. 2015, *Astrophys. J.*, 806, 183, doi: [10.1088/0004-637X/806/2/183](https://doi.org/10.1088/0004-637X/806/2/183)
- Wolstencroft, R. D., & Raven, J. A. 2002, *Icarus*, 157, 535, doi: [10.1006/icar.2002.6854](https://doi.org/10.1006/icar.2002.6854)
- Wordsworth, R. D., & Pierrehumbert, R. T. 2013, *Astrophys. J.*, 778, 154, doi: [10.1088/0004-637X/778/2/154](https://doi.org/10.1088/0004-637X/778/2/154)
- Yang, J., Abbot, D. S., Koll, D. D. B., Hu, Y., & Showman, A. P. 2019, *Astrophys. J.*, 871, 29, doi: [10.3847/1538-4357/aaf1a8](https://doi.org/10.3847/1538-4357/aaf1a8)
- Zeng, L., Jacobsen, S. B., Sasselov, D. D., & Vanderburg, A. 2018, *Mon. Not. R. Astron. Soc.*, 479, 5567, doi: [10.1093/mnras/sty1749](https://doi.org/10.1093/mnras/sty1749)